Neurosurg Rev (2017) 40:143–153
DOI 10.1007/s10143-016-0777-9

ORIGINAL ARTICLE

Fourth cranial nerve: surgical anatomy in the subtemporal transtentorial approach and in the pretemporal combined inter-intradural approach through the fronto-temporo-orbito-zygomatic craniotomy. A cadaveric study

L. Pescatori[1] · M. Niutta[1] · M.P. Tropeano[1,2] · G. Santoro[1] · A. Santoro[1]

Received: 22 June 2016 / Revised: 26 July 2016 / Accepted: 11 August 2016 / Published online: 22 August 2016

Abstract Despite the recent progress in surgical technology in the last decades, the surgical treatment of skull base lesions still remains a challenge. The purpose of this study was to assess the anatomy of the tentorial and cavernous segment of the fourth cranial nerve as it appears in two different surgical approaches to the skull base: subtemporal transtentorial approach and pretemporal fronto-orbito-zygomatic approach. Four human cadaveric fixed heads were used for the dissection. Using both sides of each cadaveric head, we made 16 dissections: 8 with subtemporal transtentorial technique and 8 with pretemporal fronto-orbito-zygomatic approach. The first segment that extends from the initial point of contact of the fourth cranial nerve with the tentorium (point Q) to its point of entry into its dural channel (point D) presents an average length of 13.5 mm with an extremely wide range and varying between 3.20 and 9.3 mm. The segment 2, which extends from point D to the point of entry into the lateral wall of the cavernous sinus, presents a lesser inter-individual variability (mean 10.4 mm, range 15.1–5.9 mm). A precise knowledge of the surgical anatomy of the fourth cranial nerve and its neurovascular relationships is essential to safely approach. The recognition of some anatomical landmarks allows to treat pathologies located in regions of difficult surgical access even when there is an important subversion of the anatomy.

Keywords Fourth cranial nerve · Skull base surgery · Tentorial segment · Cavernous segment

✉ M.P. Tropeano
mariapia.tropeano@libero.it

[1] Department of Neurology and Psichiatry-Neurosurgery, "La Sapienza" University of Rome, Viale del Policlinico 155, Rome, Italy

[2] Via Francesco Manfra n°3, 83100 Avellino, Italy

Introduction

The fourth cranial nerve, also known as the trochlear nerve, is a purely motor nerve (a somatic efferent nerve) that innervates only a single muscle: the superior oblique muscle of the eye. In some surgical approaches to the skull base, there is a significant risk of damaging the anatomical and functional entirety of this nerve. A palsy of the fourth cranial nerve affects vertical and torsional eye movements with consequent diplopia (that is maximal in the downward sight and toward the healthy side). The fourth nerve is divided into four segments: the cisternal, tentorial, cavernous, and orbital. The aim of this work, performed on cadaveric heads, is to describe the anatomy of the tentorial and cavernous segment of the fourth cranial nerve as it appears in two different surgical approaches to the skull base: the subtemporal transtentorial and the combined intra-interdural pretemporal approach to the roof and to the lateral wall of the cavernous sinus through a fronto-orbito-zygomatic craniotomy. An exhaustive anatomical analysis of the fourth nerve provides a comprehensive knowledge of its surgical anatomy and pathway.

Precise knowledge of the involved surgical anatomy is essential to safely access the anatomical regions where the

nerve runs and to minimize the risk of damage during neurosurgical procedures.

Material and methods

The anatomical study was carried out at the Laboratory of Neuroanatomy of Sapienza University of Rome. Our cadaveric study was performed on four human formalin-fixed specimens. The common carotid, the vertebral arteries, and the jugular veins were injected with red and blue colored silicone, respectively. Using both sides of each cadaveric head, we made 16 dissections: 8 with subtemporal transtentorial technique and 8 with pretemporal fronto-orbito-zygomatic approach.

Subtemporal transtentorial approach

The head has been positioned as the position of the patient during the neurosurgical procedure: parallel to the floor, and fixed in a Mayfield head-holder. An inverted u-shaped incision is made beginning at the root of the zygomatic arch approximately 1.5 cm anterior to the tragus, curving anteriorly, and upward, and then backward over the top of the ear and down to the right suboccipital region. The skin flap is reflected inferiorly, and the temporal muscle is reflected anteroinferiorly, exposing the posterior portion of the zygomatic arch as well as the zygomatic root. A temporal craniotomy is performed, measuring approximately 4 cm (height) 5 cm (width). The inferior lip of the temporal bone is either drilled down or removed with the rongeur so that there is no overhang, and the bony opening is flush with the floor of the middle cranial fossa.

The dura is opened and flapped inferiorly. Brain retractors positioned parallel are used to progressively elevate the temporal lobe until the tentorial incisura is seen. Tentorial incisura comes into view with arachnoid covering the content of the ambient cistern. The edge of the tentorium is lifted and inspected to identify where the fourth nerve enters its dural canal. Two key steps allow a degree of anterolateral reflection of the medial tentorial flap far anterolaterally that no other technique provides: (1) the critical dissection of the fourth nerve from its dural canal up to its entrance in the cavernous sinus and (2) extension of the tentorial incision up to Meckel cave (Fig.1). In summary, two retraction sutures are placed along the tentorium edge, 10 to 20 mm posterior to the fourth nerve's entrance in its dural canal, and the tentorial incision is started between both retraction sutures. After starting the incision, everting the tentorial edges and retracting the dural flap anterolaterally on 5 to 15 mm, the fourth nerve is dissected free of its dural canal for a short distance. With fine microscissors using one blade in the dural aperture and the other blade outside, the medial border of the dural canal is opened. The tentorial incision is continued and oriented toward the superior petrosal sinus at the area just over the entrance to Meckel cave. Opening of the dural tunnel proceeds in a sharp fashion by

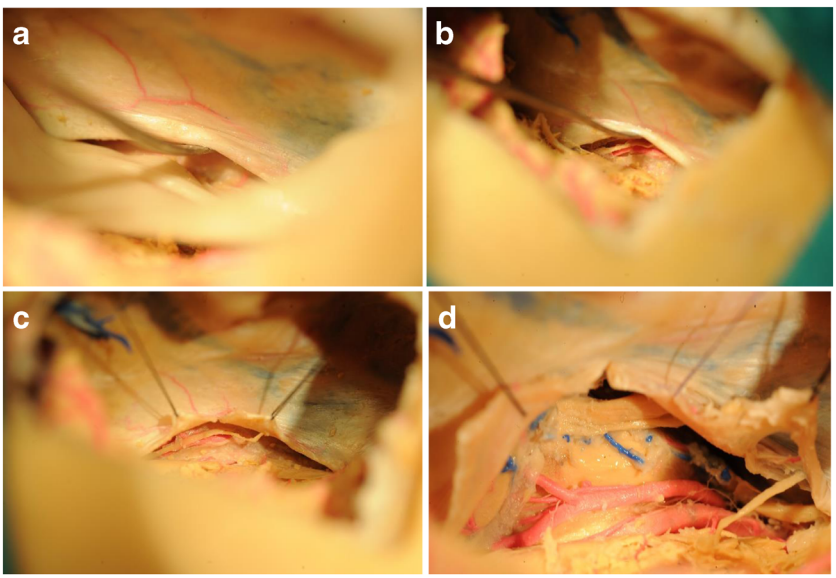

Fig. 1 **a**–**d** Left side. By a subtemporal route the free edge of the tentorium is reached with its underlying cisternal spaces (**a**). Through the careful use of a dissector the infratentorial segment of the fourth cranial nerve is identified with its entrance point in the dural canal of the tentorium (**b**). By placing two points of sutures behind the point of entrance of the IV cranial nerve in the dural canal, the tentorium is stretched and subsequently incised (**c**). By extending the incision until the superior petrosal sinus, it is possible to visualize several structures including the tentorial segment of the fourth cranial nerve, the origin of the third cranial nerve between the posterior cerebral artery, and the superior cerebellar artery as well as the origin of the fifth cranial nerve in the pons (**d**)

using the microscissors, and dissection of the fourth nerve from the canal continues in an atraumatic fashion, up to its entrance but without penetrating the cavernous sinus. The triangular tentorial flap, which includes the posterior corner of the cavernous sinus, can then be reflected far anterolaterally, if the fourth nerve is fully dissected out of its tunnel in the tentorial edge. With this technique, the fourth nerve is free of the tentorial flap, resulting in a supra- and infratrochlear working window. The dural flap is maintained in position with a stitch. In our study, the tentorial incision is extended very sideways, allowing us to see the two roots of the trigeminal nerve, sensitive, and motor, as well as the origin of the anteroinferior cerebellar artery (AICA). The segment P2 of the posterior cerebral artery (PCA), the superior cerebellar artery (SCA), and the top of the basilar artery are clearly visible.

Combined pretemporal intra and extradural approach with FTOZ craniotomy

Also in this case, the head has been positioned as the position of the patient during the neurosurgical procedure: rotated 30° slightly extended making malar prominence prominent and fixed in a Mayfield head-holder.

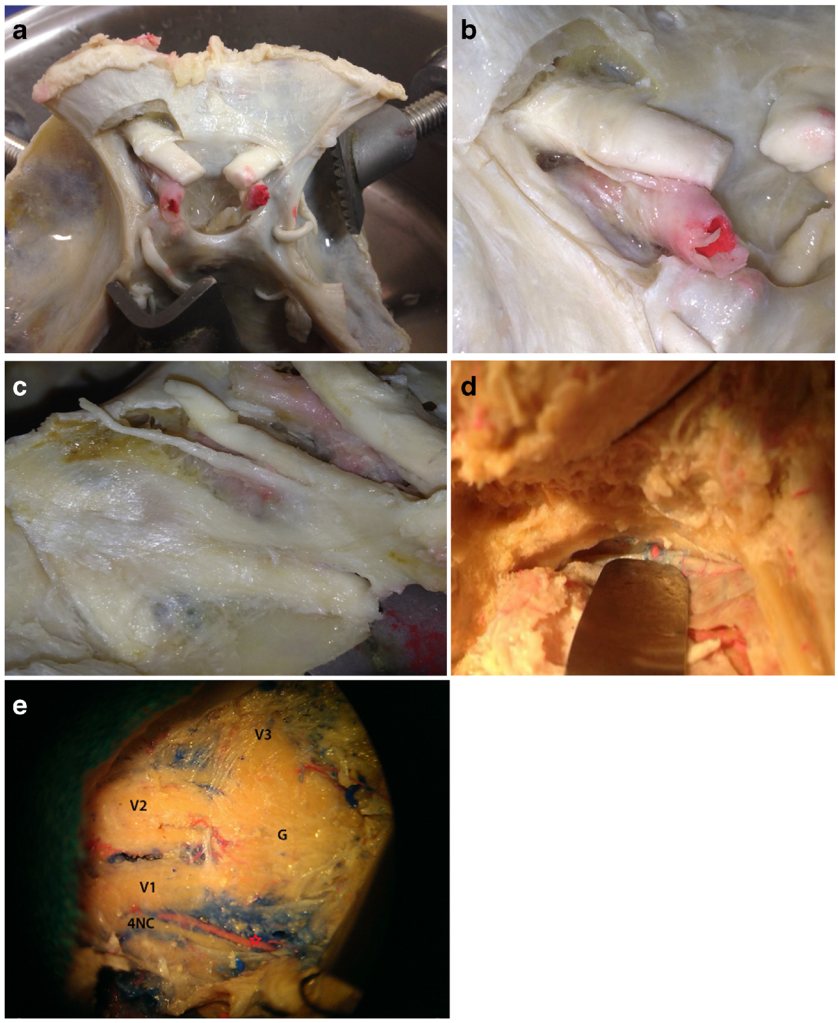

Fig. 2 **a**–**e** Sphenoid bone. The structures composing the roof of the cavernous sinus are clearly identifiable (**a**). The oculomotor triangle is constituted by the posterior and anterior petroclinoid ligament and the interclinoid ligament. The third cranial nerve enters just in the central part of the triangle. The clinoid triangle is covered by the bony prominence of the clinoid. The dura overlying the anterior clinoid forms the falciform ligament above the optic nerve as well as the diaphragm sellae. The intradural clinodectomy was performed. Magnified view of the clinoid triangle after the removal of the clinoid (**b**). It is possible to visualize the proximal and distal dural rings with the carotid collar and the carotid-oculomotor membrane. The lateral wall of the cavernous sinus after the peeling of the MCF has been completed. It is possible to visualize the third and fourth cranial nerve with the trigeminal roots V1, V2, V3, and the Gasserian ganglion (**c**). The supratroclear triangle is located between the third and fourth cranial nerve whereas the Parkinson's triangle between the fourth and V1. Intraoperative view (**d**). *Right side*. Identification of the middle meningeal artery exiting from the foramen spinosum. In this site, duplication of the middle cranial fossa dura is clearly identifiable. Intraoperative view of the lateral wall of the right cavernous sinus as it appears in the pretemporal inter-dural approach (**e**)

FTOZ craniotomy

Skin incision is made beginning at the root of the zygomatic arch, anterior to the tragus, and extending behind the hairline to the controlateral pupillary line.

Through a subgaleal dissection, the fad pad above the temporalis muscle was exposed.

An interfascial dissection of the temporal muscle was performed preserving the anatomical and functional entirety of the facial nerve. The zygomatic bone from the root to its orbital process, the lateral wall of the orbit, the orbital rim, and supraorbital nerve were gradually exposed.

The surgical technique used to complete the craniotomy was the three pieces technique with the following stages:

- Zygomatic osteotomy
- Fronto-temporal craniotomy
- Orbitotomy

At the end of the exposure, the lesser wing of the sphenoid was drilled in order to increase the basal extension of the approach.

The approach to the roof and the lateral wall of the cavernous sinus has been completed using a combination of interdural and intradural routes.

Exposure of the lateral wall and the roof of the cavernous sinus

The exposure of the lateral wall of the cavernous sinus was obtained through the interdural dissection (Fig.2).

Two essential landmarks were identified for the peeling of the middle cranial fossa (MCF): the meningo-orbital ligament and the middle meningeal artery exiting from the foramen spinosum. In order to expose the areas of cleavage of the dural sheets, both these two structures were incised through microscissors. The dissection was performed in rostrum-caudal sense exposing gradually the lower edge of the third cranial nerve, the fourth nerve, roots V1, V2, V3, the Gasserian ganglion, and the greater petrosal superficial nerve (GPSN).

Subsequently, once the dura mater had been opened, the anterior clinoid was removed intradurally releasing the clinoid process from the lesser wing of the sphenoid, the sphenoid planum, and finally drilling the optic strut. Once the anterior clinoid process removal and the dissection of the proximal and distal dural rings as well as the carotid-oculomotor membrane had been completed, it was possible to expose both the clinoid and the oculomotor triangle of the roof of the cavernous sinus with the third cranial nerve.

At the end of the dissection, both the lateral wall and the roof of the sinus were clearly exposed with their constituting triangles.

Measurements

After finishing both dissections on the same side, it was possible to appreciate the continuity of the cisternal, tentorial, and cavernous segments of the fourth cranial nerve.

By the identification of specific anatomical landmarks, detailed measurements of the anatomical structures exposed were performed using a microscopic centesimal scale caliper with a flow rate of 20 cm and sensitivity of 0.05 mm without traumatic manipulations.

The purpose of the measurements was to quantify the length of the different segments of the cisternal and infratentorial portion of the fourth cranial nerve and the area of the oculomotor, supratrochlear, and infratrochlear triangles (Fig.3, Fig.4).

The anatomical landmarks chosen to take measurements were the following:

T: point where the third nerve came into contact with the tentorial edge
Q: point where the fourth nerve first came into contact with the tentorial edge
D: the point where the fourth nerve pierced the tentorial dura

Segment 1: distance QD
Segment 2: distance from D to the point where the fourth nerve reached the cavernous sinus

For a complete characterization of the course of the nerve, we also made the following measurements:

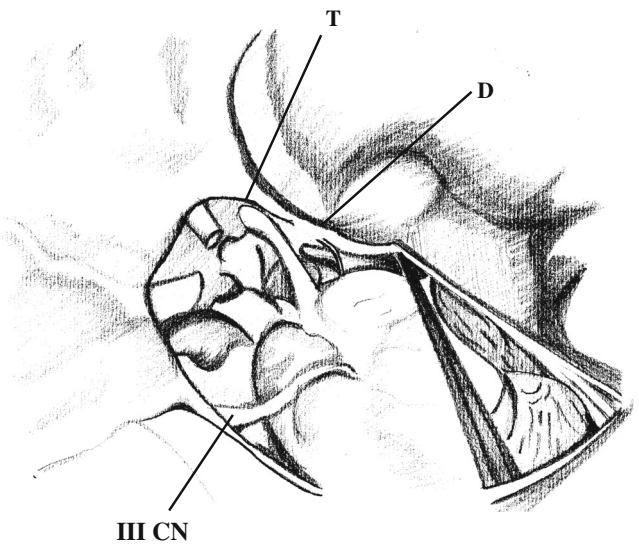

Fig. 3 Schematic drawing, superolateral view. The picture illustrates the relationship of the trochlear nerve with the tentorium. Superolateral view. The point of contact/of entrance in the tentorium can be visualized on the right side. From this point of view, it is possible to evaluate the distance between the point D to the point in which the oculomotor nerve contacts the free tentorial edge (*T*)

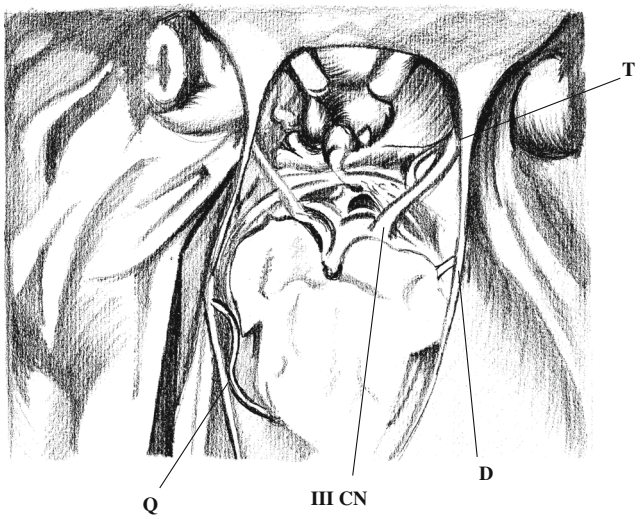

Fig. 4 Schematic drawing, superior view. In this picture, it is possible to appreciate the first point of contact of the fourth cranial nerve with the tentorium, the point of entrance into the tentorial dural ring, and the point of contact of the third cranial nerve with the free tentorial edge. The length of the different segment can be induced by identifying these points

- Segment TQ: the distance between the point where the oculomotor nerve came into contact with the free tentorial edge cerebelli and the point where the fourth nerve came into contact with the tentorial edge
- Segment TD: the distance between the point where the third nerve came into contact with the tentorial edge and the point where the fourth nerve pierced the tentorial dura
- Transverse distance between medial edge of the trigeminal nerve and the fourth nerve on the superior petrosal border (attached margin of the tentorium)

The triangles of the cavernous sinus were defined by the following anatomical landmarks:

The medial and lateral edges of the Fukushima's triangle [1] or supratrochlear triangle are, respectively, the lower surface of the oculomotor nerve and the upper surface of the fourth nerve; the base of the triangle is the dura that extends between the points where the third and fourth cranial nerve begin to run within the lateral wall of the cavernous sinus.

The Parkinson's triangle [2], also called the infratrochlear triangle, is located finding the lower edge of the fourth nerve from where it begins to run in the lateral wall cavernous sinus to the point where it enters the orbit through the superior orbital fissure and then looking for the upper edge of V1. The base of the triangle is the line connecting the points of entry of the two nerves in the lateral wall of the cavernous sinus.

Finally, the median edge of the oculomotor triangle has been identified by the line passing between the center of the anterior and posterior clinoid process (interclinoid ligament); the base is the thickening dura that form the posterior petroclinoid ligament and the anterior petroclinoid ligament.

In this study, we used the Rhoton's nomenclature [3].

For the calculation of the area of the triangles of the cavernous sinus was applied Heron's formula:

$$A = \sqrt{p.(p-a).(p-b).(p-c)}$$

where a, b, and c are the three sides of the triangle, and p is the semi-perimeter:

$$p = \frac{a+b+c}{2}$$

The choice of using Heron's formula derives from the immediacy of the known resolution of the triangle sides, without resorting to trigonometric calculations that would have required the measurement of angles.

Results

The results of our study are summarized in Tables 1, 2, 3, and 4.

The length of segment 1 (QD) varied from 20.3 to 9.3 mm, with a mean value of 13.5 mm (SD 4.1). Segment 2 ranged from a maximum value of 15.1 mm to a minimum of 5.3, with a mean of 9.8 (SD 3.1). Mean length of segment TD was 9.8 (14.3–5.3 mm, SD 3.1). The maximum length of segment TQ was 30.1 mm, whereas its minimum value was 21.9 mm (mean 21.9, SD 5.5).

Table 1 Length of segment 1 and 2 and the distance between point T, D, and Q

n°	Segment 1 (mm)		Segment 2 (mm)		TD (mm)		TQ (mm)		Petrous sinus (mm)	
1	20.3		15.1		14.3		30.1		7.1	
2	18.1		14.2		12.8		27.2		6.9	
3	15.7		12.1		11.6		25.7		5.2	
4	12.4	Mean	11.6	Mean	10.1	Mean	23.4	Mean	4.1	Mean
5	11.9	**13.5125**	9.2	**10.4**	9.5	**9.775**	19.2	**21.9**	3.5	**3.825**
6	11.3		8.3		7.4		17.9		2.6	
7	9.1	SD	6.8	SD	7.2	SD	16.5	SD	1.2	SD
8	9.3	4.103113	5.9	3.378926	5.3	3.057427	15.2	5.468873	0	2.543198

Table 2 Length of segment 1 and 2 and the distance between point T, D, and Q

8 cases	Maximum value (mm)	Minimum value (mm)	Mean (mm)	Standard deviation
Segment 1 (QD)	20.3	9.3	13.5	4.1
Segment 2	15.1	5.9	10.4	3.4
Distance TD	14.3	5.3	9.8	3.1
Distance TQ	30.1	15.2	21.9	5.5

The mean values of the edges of the clinoid triangle were 7.58 mm for the medial edge, 12.65 for the lateral edge and 8.63 for the base. Mean area of the clinoid triangle was 32.1 mm.

The infratrochlear or Parkinson's triangle mean area was 22.6 mm. Its medial edge had a mean length of 10.2; its lateral edge mean length was 12.17 mm whereas its base measured an average of 4.57 mm.

Table 3 Triangles' area (a, b, and c)

Clinoid triangle (mm)							
n°	a		b		c		Area
1	9.1		14.8		10.2		32.02051
2	8.5	Mean	14.2	Mean	9.5	Mean	
3	8.2	7.5875	13.9	12.65	9.4	8.6375	
4	7.9		13.8		9.1		
5	7.2	SD	12.5	SD	8.5	SD	
6	7.1	1.031556	11.3	1.791249	8.3	1.146345	
7	6.8		10.6		7.2		
8	5.9		10.1		6.9		

(a)

Infratrochlear triangle (mm)							
n°	a		b		c		Area
1	12.1		14.6		5.1		22.59627
2	11.6	Mean	13.5	Mean	5	Mean	
3	10.9	10.2	12.6	12.175	4.9	4.575	
4	10.5		12.4		4.8		
5	10.3	SD	11.9	SD	4.5	SD	
6	9.2	1.369046	11.6	1.443953	4.3	0.443203	
7	8.8		10.5		4.1		
8	8.2		10.3		3.9		

(b)

Supratrochlear triangle (mm)							
n°	a		b		c		Area
1	15.6		16.1		6.2		33.10398
2	14.9	Mean	15.8	Mean	5.9	Mean	
3	13.6	12.975	14.5	14.3875	5.8	5.125	
4	12.8		14.2		5.1		
5	12.4		13.9		4.9		
6	11.9	SD	13.7	SD	4.6	SD	
7	11.5	1.61223	13.6	1.034322	4.3	0.762983	
8	11.1		13.3		4.2		

(c)

a, b, and c are the sides of the triangles. The mean and the SD of each side have been highlighted with colors (red for a, yellow for b, and blue for c) for a better and easier comprehension of the tables

Table 4 Comparison between triangles' area

Triangle	Medial edge (mm)	Standard deviation	Lateral edge (mm)	Standard deviation	Base (mm)	Standard deviation	Area (mm2)
Clinoid	7.58	1.03	12.65	1.79	8.63	1.15	32.1
Infratrochlear	10.2	1.36	12.17	1.44	4.57	0.44	22.6
Supratrochlear	12.97	1.61	14.38	1.03	5.13	0.76	33.1
Oculomotor	12.05	0.98	17.37	0.96	11.02	0.83	65.84

Fukushima's triangle mean area was 33.1 mm. The mean values of the margins of this triangle were 12.97 for the medial edge, 14.38 for the lateral edge, and 5.13 for its base.

The mean length of the edges of the oculomotor triangle was 12.05 mm for the medial edge, 17.37 mm for the lateral edge, and 11.02 for the base. Mean area of the oculomotor triangle was 65.84 mm.

Discussion

Traditionally, the fourth nerve is divided into three segments: cisternal, cavernous, and orbital. Some authors describe also the tentorial segment [4–7].

Iaconetta et al. [8] divided the fourth nerve into five segments: cisternal, tentorial, cavernous, fissural, and orbital.

Recently, Tubbs RS et al. [6] described another segment. This is called the "trigonal" segment that develops from the point where the nerve enters the back corner of the oculomotor trigone up to the lateral wall of the cavernous sinus.

The purpose of the different classifications is to provide a detailed description of the anatomy of a structure that is exposed to a high risk of damage in the skull base surgery.

Surgical approaches described in our study are among the most risky as regard to this possibility.

In the subtemporal transtentorial approach, the risk of damaging the fourth cranial nerve is high in manipulation and incision of the free edge of the tentorium because it hides the infratentorial portion of the nerve by direct surgical visualization.

In the pretemporal approach to the lateral wall and the roof of the cavernous sinus, knowledge of the correct localization of the nerve is essential to prevent its damage in the maneuver of peeling of the middle cranial fossa (MCF) as well as in the removal of lesions involving the lateral wall of the sinus (Meckel's meningiomas, neuromas of fifth nerve) or in the treatment of aneurysms of the internal carotid artery.

In literature, cisternal, cavernous, and orbital segments of the fourth nerve are widely described; conversely, studies of the tentorial segment are not common.

Based on Tulika Gupta et al.'s studies [9], we have described the anatomy of the tentorial portion of the fourth nerve and performed our measurements from the surgical perspective of the subtemporal transtentorial approach comparing the data of surgical dissection with those of anatomical dissections performed in the above mentioned work. Results obtained in our study confirmed those reported in literature.

By simulating the surgical approach, it was possible to verify the usefulness and applicability of the data obtained in our measurements. Of particular practical use, it proved to be the subdivision of the tentorial portion of the fourth tentorial cranial nerve into two segments.

The first segment that extends from the initial point of contact of the fourth cranial nerve with the tentorium (point Q) to its point of entry into its dural channel (point D), presents an average length of 13.5 mm with an extremely wide range and varying between 20.3 and 9.3 mm. Given the wide interindividual variability of this stretch and its easy deformability by pathological compressions, morphometric data of this segment do not show a significant surgical applicability.

Conversely, the segment 2, which extends from point D to the point of entry into the lateral wall of the cavernous sinus, presents a lesser interindividual variability (mean 10.4 mm, range 15.1–5.9 mm) and an anatomical course less deformable by pathological compressions because its localization within a relatively rigid structure as the tentorium. This aspect makes the second segment of the fourth nerve a valuable aid for the neurosurgeon in this type of approach and in the lesions at the

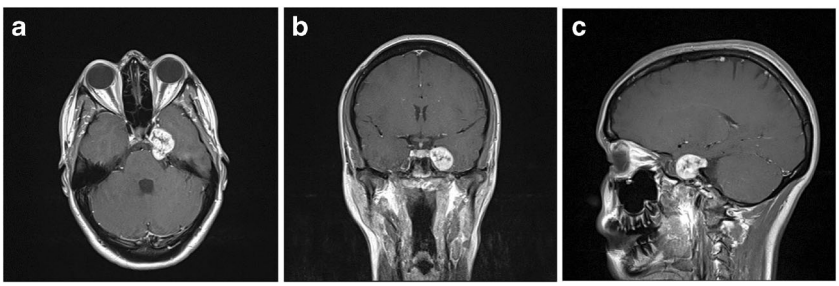

Fig. 5 **a**–**c** Preoperative MRI showing the presence of a lesion disomogeneously enhancing after administration of gadolinum located within the Meckel's cave and partially extending in the posterior cranial fossa following the fifth nerve root

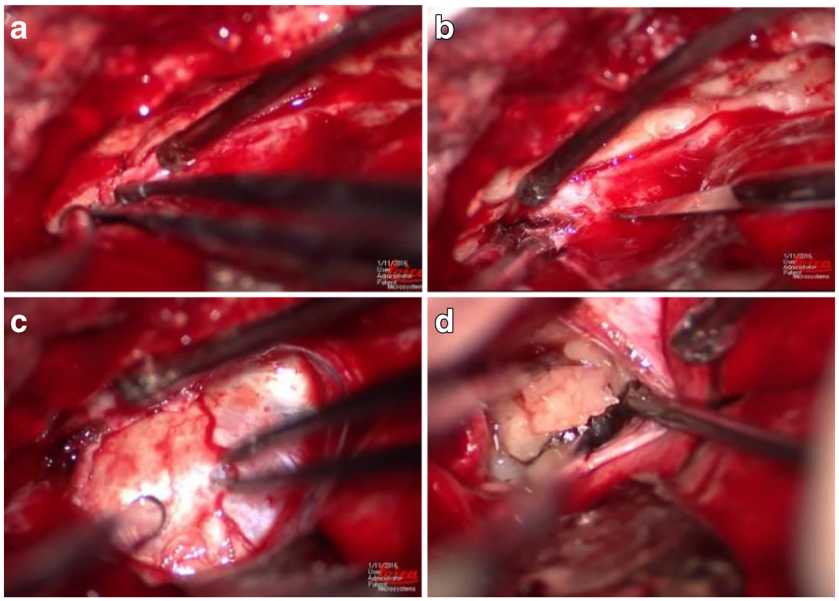

Fig. 6 **a–d** Intraoperative view. Identification of the middle meningeal artery and coagulation. Peeling of the middle fossa. In this case, we decided to incise the dura in order to remove the portion of the lesion located in posterior cranial fossa. Exposition of the tumor and microsurgical removal

tentorial incisura. In fact, after identifying the point T of contact between the third cranial nerve and the tentorial dura, it is possible to predict with good approximation the entry point of the fourth cranial nerve inside the tentorium even in those cases in which the presence of pathological lesions make difficult or not possible the visualization of the nerve itself. According to our measurements, the maximum value of this distance is 14.3 mm. As a consequence, performing the tentorial incision approximately 1.5 cm behind the point T, the risk of injuring the fourth nerve is significantly reduced.

With regard to the modified technique of engraving the tentorium that we used, a net gain of exposure of at least 5 mm in rostro-caudal direction (range, 2.9–7.9 mm; SD 1.9 mm) with a surgical window expansion of about 150 % (from 120 to 183 %) is described in literature [8, 10]. Our study confirms thess results, even if with a slightly narrower range. We have in fact found a net gain exposure of 5.25 mm (between 3.8 and 6.7 mm).

Similar considerations to those previously mentioned for the subtemporal transtentorial approach can be made for the pretemporal approach to the lateral wall and the roof of the cavernous sinus.

Tumoral lesions localized in the MCF as meningiomas of the Meckel's cave and neuromas of the fifth nerve as internal carotid artery ICA aneurysms may cause alterations of the morphology of the lateral wall and the roof of the cavernous sinus making difficult to recognize neurovascular structures of the region. However, although the degrees of morphological distortion can be significant, the recognition of the structure of the triangles of the cavernous sinus is still possible for the surgeon who has received an adequate neuroanatomical training. This significantly decreases the risk of damaging functionally important structures, including the fourth cranial nerve, in the treatment of lesions in this region [11]. The oculomotor triangle is the area in which the third cranial nerve enters into the roof of the cavernous sinus and is defined by the anterior and posterior petroclinoid ligaments and interclinoid ligament. This space, that in our study measures 65.84 mm^2, is very important, in fact provides a useful passageway for the achievement of the distal portion of the intracavernous ICA. It is also useful for approaches to interpedicular fossa and tumors involving the medial portion of the cavernous sinus.

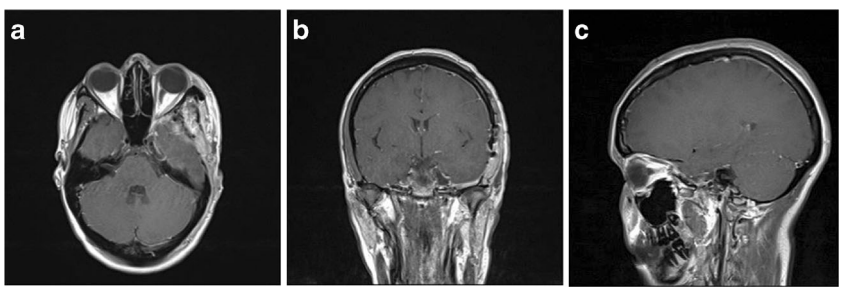

Fig. 7 **a–c** Postoperative MRI showing the complete removal of the lesion

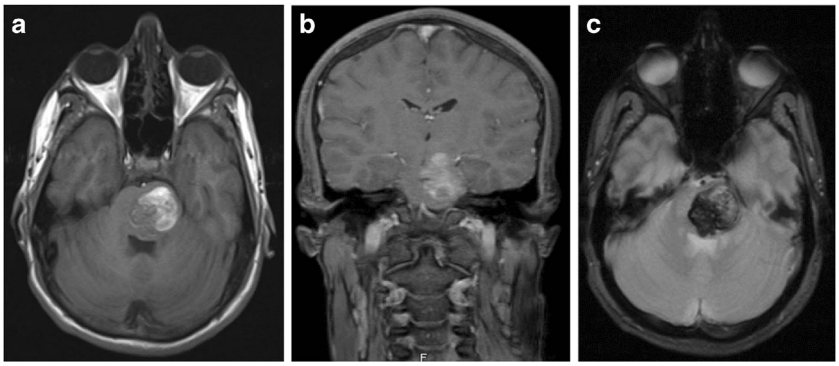

Fig. 8 **a**–**c** T1 weighted MRI showing the presence of a bleeding lesion in the pons in the axial and coronal planes. Gradient echo showing the characteristic appearance of the bleeding cavernoma

The supratrochlear triangle is a strategic point in which the surgeon can expose the posterior bend of the intracavernous tract of ICA, as well as the origin of the meningohypophyseal trunk [3, 12, 13]. In our study, triangle's area measures 33.10 mm^2.

The Parkinson's (infratrochlear) triangle includes the meningohypophyseal trunk and the posterior bend of the ICA in most cases, except for those variants in which the artery is very tortuous [3]. Moreover, it allows the exposure of the sixth cranial nerve [7]. The area measures 22.60 mm^2.

It is a narrow space, which can be expanded through a dissection and displacement of V1 and fourth nerve [7].

The characterization of the triangles of the anterior region of the cavernous sinus acquires a central role in defining the microanatomy of fourth nerve, goal of our study.

The oculomotor, the infratrochlear, and the supratrochlear triangle, as well as the clinoid triangle, are passageways exploitable for the treatment of multiple lesions involving the cavernous sinus and adjacent areas and for this reason is required a precise knowledge of the location and the size of these spaces. This is the reason that led us to carry out measurements as detailed in this region.

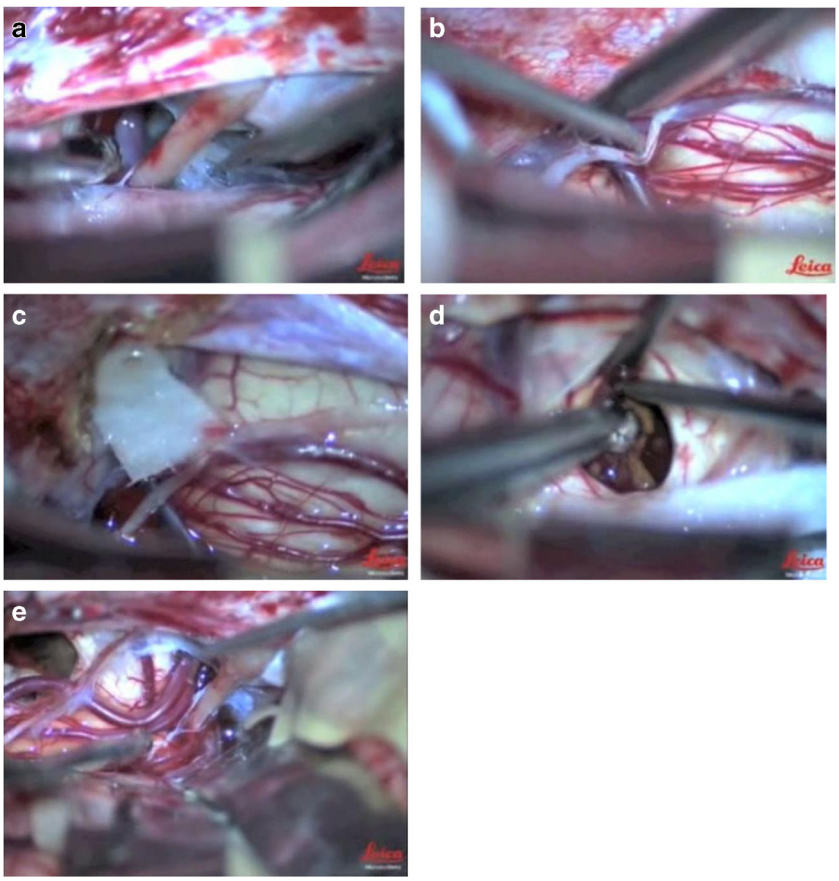

Fig. 9 **a**–**e** Intraoperative view. Identification of the point in which the third cranial nerve contact the tentorium (**a**). Identification of the fourth cranial nerve located within the ambient cistern beneath the tentorium (**b**). Removal of the cavernoma located in the pons (**c**, **d**). Surgical field after the removal of the lesion. The origin of the third cranial nerve in the interpeduncular fossa is clearly appreciable between the SCA and PCA. Behind the fourth cranial nerve crosses the surgical field (**e**)

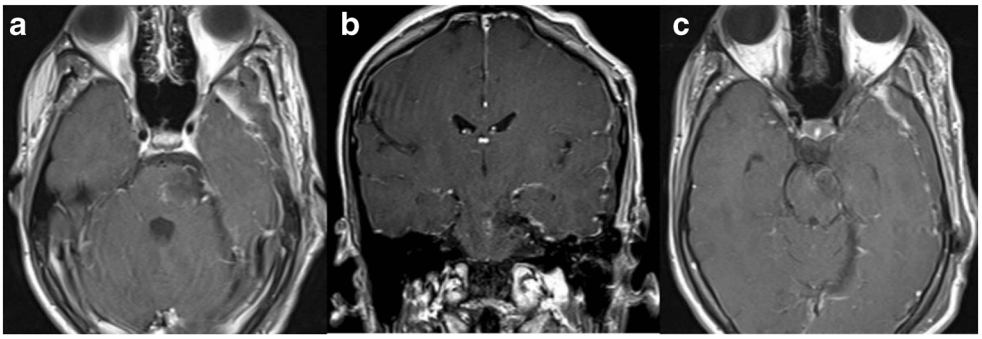

Fig. 10 **a**–**c** Postoperative MRI showing the complete removal of the lesion

Illustrative cases

We have selected some clinical cases to illustrate successful surgical strategies for removing lesions located in areas reachable through the approaches above described.

Illustrative case 1

The first case is a 15-year-old boy who was recovered at our department after the onset of mild right hemiparesis and periferic facial palsy. The MRI showed an extended area of altered signal intensity, heterogeneously hypo-hyperintense in T1 localized at pons and mesencephalon that could be related to a cavernoma with evidence of recent bleeding (Fig.5).

Because of the lesion location, the patient underwent subtemporal transtentorial approach (Fig.6).

The lesion was completely removed (Fig.7). Histological examination confirmed the suspect of cavernoma. Postoperative course was uneventful. Patient was discharged after 10 days. Facial nerve palsy and hemiparesis slowly recovered during the next few months.

Illustrative case 2

A 20-year-old girl presented a mild left trigeminal hypoesthesia. An MRI scan showed the presence of a pathological tissue heterogeneously hyperintense in T2 localized in the Meckel's cave and along the cisternal segment of the V cranial nerve (Fig.8). A combined pretemporal intra and extradural approach with fronto-temporo-orbito-zygomatic (FTOZ) craniotomy (Fig.9). The lesion was completely removed (Fig.10). Histological examination revealed a trigeminal Schwannoma. Postoperative course was uneventful. Trigeminal hypoestesia did not worse after the procedure. Patient was discharged in fifth postoperative day.

Conclusion

In conclusion, in the performance of subtemporal transtentorial approaches and pretemporal FTOZ for the treatment of pathologies located at tentorial incisura and at the lateral wall and the roof of the cavernous sinus, there is the possibility that the surgeon encounters an important subversion of the normal anatomy, due to expansive lesions, vascular lesions, as large aneurysms, that can create significant problems of identification of anatomical structures as the fourth NC.

Nevertheless, there are some relatively fixed anatomical landmarks that allow the neurosurgeon to orient himself during the procedure, although the anatomy is altered. The recognition of these anatomical landmarks allows to treat pathologies located in regions of difficult surgical access limiting the risk of damaging functionally important structures as the fourth cranial nerve.

Acknowledgments This article was written in memory of Dr. M. Niutta, a student of medicine who contributed with the first author to the dissections. He disappeared few days before discussing the results of this work on his graduation day. The efforts profused for the publication of this study are entirely dedicated to him and to his incredible family.

Moreover, we would like to acknowledge Mrs. A. Giglioni for her wonderful drawings.

Funding No funding was received for this research.

Conflict of interest All authors certify that they have no affiliations with or involvement in any organization or entity with any financial interest (such as honoraria; educational grants; participation in speakers' bureaus; membership, employment, consultancies, stock ownership, or other equity interest; and expert testimony or patent-licensing arrangements) or non-financial interest (such as personal or professional relationships, affiliations, knowledge, or beliefs) in the subject matter or materials discussed in this manuscript.

Ethical approval All procedures performed in studies involving human participants were in accordance with the ethical standards of the institutional and/or national research committee and with the 1964 Helsinki declaration and its later amendments or comparable ethical standards.

Informed consent Informed consent was obtained from all individual participants included in the study.

References

1. Day JD, Fukushima T, Giannotta SL (1994) Microanatomical study of the extradural middle fossa approach to the petroclival and posterior cavernous sinus region: description of the rhomboid construct. Neurosurgery 34(6):1009–1016
2. Parkinson D (1965) A surgical approach to the cavernous portion of the carotid artery. Anatomical study and case report. J Neurosurg 23(5):474–483
3. Rhoton AL Jr (2002) The supratentorial cranial space: microsurgical anatomy and surgical approaches. Neurosurgery 51(4):S1
4. Ammirati M, Musumeci A, Bernardo A, Bricolo A (2002) The microsurgical anatomy of the cisternal segment of the fourth nerve, as seen through different neurosurgical operative windows. Acta Neurochir 144:1323–1327
5. Bisaria KK (1988) Cavernous portion of the trochlear nerve with special reference to its site of entrance. J Anat 159:29–35
6. Tubbs RS, Veith P, Griessenauer CJ, Loukas M, Cohen-Gadol AA (2014) A new segment of the trochlear nerve: cadaveric study with application to skull base surgery. J Neurol Surg B Skull Base 75(1): 8–10
7. Dolenc VV (2003) Microsurgical anatomy and surgery of the central skull base. Springer-Verlag, Wien
8. Iaconetta G, de Notaris M, Benet A, Rincon J, Cavallo LM, Prats-Galino A, Samii M, Cappabianca P (2013) The trochlear nerve: microanatomic and endoscopic study. NeurosurgRev 36:227–238
9. Gupta T, Gupta SK, Sahni D. (2014) Anatomy of the tentorial segment of the trochlear nerve in reference to its preservation during surgery for skull base lesions. Surg Radiol Anat
10. McLaughlin N, Ma QF, Emerson J, Malkasian DR, Martin NA (2013) The extended transtentorial approach: the impact of trochlear nerve dissection and tentorial incision. J Clinical Neuroscience 20:1139–1143
11. Al-Mefty O (1989) Surgery of the cranial base surgery. KluwerAcademia Publishers, Boston
12. DayJD (1996) Microsurgical dissection of the cranial base. Churchill Livingstone, New York
13. Harris FS, Rhoton AL Jr (1976) Anatomy of the cavernous sinus: amicrosurgical study. J Neurosurg 45:169–180